Autonomic Denervation With Magnetic Nanoparticles

Lilei Yu, Benjamin J. Scherlag, Kenneth Dormer, Kytai T. Nguyen, Carey Pope, Kar-Ming Fung and Sunny S. Po

Circulation 2010, 122:2653-2659: originally published online December 6, 2010
doi: 10.1161/CIRCULATIONAHA.110.940288
Circulation is published by the American Heart Association. 7272 Greenville Avenue, Dallas, TX 72514
 Print ISSN: 0009-7322. Online ISSN: 1524-4539

Autonomic Denervation With Magnetic Nanoparticles

Lilei Yu, MD; Benjamin J. Scherlag, PhD; Kenneth Dormer, PhD;
Kytai T. Nguyen, PhD; Carey Pope, PhD; Kar-Ming Fung, MD, PhD; Sunny S. Po, MD, PhD

Background—Prior studies indicated that ablation of the 4 major atrial ganglionated plexi (GP) suppressed atrial fibrillation.

Methods and Results—Superparamagnetic nanoparticles (MNPs) made of Fe_3O_4 (core), thermoresponsive polymeric hydrogel (shell), and neurotoxic agent (N-isopropylacrylamide monomer [NIPA-M]) were synthesized. In 23 dogs, a right thoracotomy exposed the anterior right GP (ARGP) and inferior right GP (IRGP). The sinus rate and ventricular rate slowing responses to high-frequency stimulation (20 Hz, 0.1 ms) were used as the surrogate for the ARGP and IRGP functions, respectively. In 6 dogs, MNPs carrying 0.4 mg NIPA-M were injected into the ARGP. In 4 other dogs, a cylindrical magnet (2600 G) was placed epicardially on the IRGP. MNPs carrying 0.8 mg NIPA-M were then infused into the circumflex artery supplying the IRGP. The hydrogel shell reliably contracted in vitro at temperatures ≥37°C, releasing NIPA-M. MNPs injected into the ARGP suppressed high-frequency stimulation–induced sinus rate slowing response (40±8% at baseline; 21±9% at 2 hours; $P=0.006$). The lowest voltage of ARGP high-frequency stimulation inducing atrial fibrillation was increased from 5.9±0.8 V (baseline) to 10.2±0.9 V (2 hours; $P=0.009$). Intracoronary infusion of MNPs suppressed the IRGP but not ARGP function (ventricular rate slowing: 57±8% at baseline, 20±8% at 2 hours; $P=0.002$; sinus rate slowing: 31±7% at baseline, 33±8% at 2 hours; $P=0.604$). Prussian Blue staining revealed MNP aggregates only in the IRGP, not the ARGP.

Conclusions—Intravascularly administered MNPs carrying NIPA-M can be magnetically targeted to the IRGP and reduce GP activity presumably by the subsequent release of NIPA-M. This novel targeted drug delivery system can be used intravascularly for targeted autonomic denervation. **(*Circulation*. 2010;122:2653-2659.)**

Key Words: arrhythmia ■ atrial fibrillation ■ nervous system, autonomic ■ magnetic nanoparticles

Catheter ablation has become a mainstay treatment for drug-refractory atrial fibrillation (AF). However, the success of ablation has been limited by insufficient understanding of the mechanisms underlying the initiation and maintenance of AF. Prior studies on spontaneous initiation of AF in patients and animals indicated that activation of both the sympathetic and parasympathetic nervous systems often preceded the onset of AF.[1–4] Mammalian hearts are dually innervated by the extrinsic and intrinsic cardiac autonomic nervous system. The intrinsic cardiac autonomic nervous system is a neural network composed of several ganglionated plexi (GP) and interconnecting nerves and/or neurons.[5–7] GP serve as the "integration centers" in this neural network. Multiple studies have shown that chemical or electric stimulation of the GP can initiate rapid firing from the pulmonary vein (PV) or PV-atrial junction, resembling the focal firing observed in a patient with AF.[8,9] Ablation of the major atrial GP suppressed the inducibility and maintenance of AF in animals.[10,11] Recent clinical studies also demonstrated that GP ablation as an adjunct therapy to PV isolation improved the outcome of AF ablation, whereas GP ablation alone produced a success rate similar to the standard PV isolation.[12–17] This denervation-only ablation strategy has the advantage of producing more focused lesion sets and potentially carrying a smaller risk of producing iatrogenic macroreentrant left atrial tachycardia.

Editorial see p 2642
Clinical Perspective on p 2659

Targeted drug delivery is an emerging technology in which therapeutic delivery to tissues can increase drug efficacy, alleviate side effects, and reduce costs. Polymeric nanoparticles with sizes that range from 10 to 200 nm can be formulated with absorbed, attached, or encapsulated drugs for burst and/or controlled release.[18–22] In the present study, to achieve the goal of targeted drug deliver to the GP to treat AF, we synthesized and functionalized superparamagnetic nanoparticles (MNPs) containing magnetite (core), a thermoresponsive hydrogel matrix (shell), and a payload. A neurotoxic agent, *N*-isopropyl acrylamide monomer (NIPA-M),

Received January 2, 2010; accepted October 1, 2010.

From the Department of Cardiology, Renmin Hospital of Wuhan University, Wuhan, China (L.Y.); Department of Medicine and Heart Rhythm Institute (L.Y., B.J.S., S.S.P.), Department of Physiology (K.D.), and Department of Pathology (K.-M.K.), University of Oklahoma Health Sciences Center, Oklahoma City; Department of Bioengineering, University of Texas at Arlington, Arlington, Texas (K.T.N.); and Department of Physiological Sciences, College of Veterinary Medicine, Oklahoma State University, Stillwater (C.P.).

Correspondence to Sunny S. Po, MD, PhD, 1200 Everett Dr, Room TUH6E103, Oklahoma City, OK 73104. E-mail sunny-po@ouhsc.edu

Circulation **is available at http://circ.ahajournals.org** **DOI: 10.1161/CIRCULATIONAHA.110.940288**

was incorporated into a hydrogel matrix as the payload. In the presence of an external magnetic field, this construct enabled magnetic capture of the MNP at the targeted GP site and allowed the payload (NIPA-M) to be released to ablate the neural elements in the targeted GP.

Methods

Synthesis and Functionalization of MNPs

To synthesize MNPs, the core (magnetite, Fe_3O_4) was formed by coprecipitation of ferrous and ferric salts in the presence of basic solution and docusate sodium salt as a surfactant developed previously.[23,24] Then, the magnetic nanoparticles were coated with vinyltrimethoxysilane via acid catalyst hydrolysis followed by electrophilic substitution on the surface of the MNPs.[24–27] Poly-*N*-isopropylacrylamide-coacrylamide (pNIPA-AAm), a thermoresponsive hydrogel, was then polymerized on the magnetic core via a silane coupling agent and radical polymerization method. This process allows a strong attachment of the magnetic core with the polymeric hydrogel matrix (shell), thereby preventing the core of the MNP from diffusing out of the polymer shell and permits the encapsulation of a therapeutic payload (NIPA monomer, NIPA-M). The lower critical solution temperature of the hydrogel, the temperature above which the hydrogel contracts and disintegrates, used in the present study was formulated at 37°C, allowing enhanced drug release only at body temperature. Of note, although the polymeric NIPA (pNIPA-AAm) was an essential element of the hydrogel shell of our nanoparticles, pNIPA-AAm, unlike NIPA-M, is not neurotoxic.[28]

The size of the pNIPA-AAm–coated MNPs was evaluated by transmission electron microscopy and a laser scattering particle sizer as previously described.[24] To assess the temperature sensitivity of our polymer shell, optical transmittance of the MNP solution (2 mg/mL) at various temperatures (15°C to 50°C at a rate of 1°C/min) was measured at 650 nm with a Cary-50 UV-Vis spectrophotometer (Agilent, Lexington, MA), which was coupled with a PCB-150 circulating water bath as described previously.[24,25]

For drug loading, the freeze-dried pNIPA-AAm–coated MNPs (2.5 mg/mL) were resuspended and incubated with NIPA-M (drug; 2.5 mg/mL) in PBS at 4°C for 3 days on a shaker. After incubation, drug-loaded MNPs were collected with a magnet. The supernatant was stored at −20°C for determination of loading efficiency indirectly. The loading efficiency is defined as the difference between the total amount of added NIPA-M and the amount present in the supernatant divided by the total amount of added NIPA-M.[29]

To study the drug release kinetics of NIPA-M, nanoparticles were suspended in PBS solution at 25°C and 37°C for 14 days on a shaker with gentle mixing. At designated time intervals, MNPs were captured against the side of a tube by a magnet, and the supernatant was removed from each sample and stored at −20°C for later analysis. After experiments, the amount of NIPA-M was determined as described previously.[29] In brief, a UV-Vis spectrophotometer was used for the measurement of NIPA-M released from the nanoparticles over the time. To generate a standard curve of NIPA-M concentrations against the absorbance, NIPA-M standards were prepared by dissolving a known amount of NIPA-M in PBS and by preparing serial dilutions. The NIPA-M standards and NIPA-M released in each sample (200 μL) were added to a 96-well plate (transparent and compatible for UV wavelengths). The plate was read at 270 nm for absorbance with a UV-Vis spectrophotometer. The standard curve was plotted and the absorbance readings of samples were determined against the standard curve. Finally, the NIPA-M release curve, cumulative NIPA-M release (percent of loading) versus time (hours), was plotted.

Animal Preparation and In Vivo Studies

Twenty-three adult mongrel dogs weighing 20 to 25 kg were anesthetized with sodium pentobarbital. Positive pressure ventilation was instituted with a respirator. Core temperature was maintained at 37.0±1.0°C. The chest was opened via a right lateral thoracotomy at the fourth intercostal space. The pericardium was incised and reflected to expose the right atrium (Figure 1). Electrograms were recorded from the His bundle region, right atrium, and right superior and inferior PVs. At the base of the right PVs adjacent to the caudal end of the sinoatrial node, there is a distinct fat pad known to contain the anterior right ganglionated plexus (ARGP). At the junction of the inferior vena cava and both atria, there is a fat pad that contains the inferior right GP (IRGP). High-frequency stimulation (20 Hz, 0.1 ms, square pulse) was applied to both GP at the voltage level that did not excite the atrium through a 2-channel Grass stimulator (S88; Astro-Med, Warwick, MA) as previously described.[30] Prior studies have shown that the ARGP function could be assessed by the sinus rate slowing response elicited by ARGP stimulation, whereas the IRGP function could be assessed during AF by the ventricular rate slowing response induced by IRGP stimulation.[31,32] At higher voltage levels, which varied from animal to animal, AF could be induced by stimulation of the ARGP or IRGP. The lowest voltage required to induce AF was determined to be the inducibility threshold for each dog. AF is defined as an irregular atrial rate >500 bpm associated with irregular atrioventricular conduction.

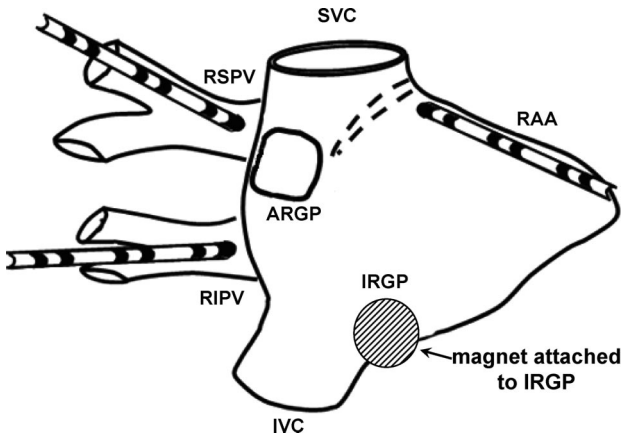

Figure 1. Diagrammatic representation of the atria as seen from a right-sided thoracotomy. Electrode catheters were sutured at the right superior and right inferior PVs (RSPV and RIPV, respectively) and on the right atrial appendage (RAA). SVC indicates superior vena cava; IVC, inferior vena cava.

In 6 animals, 0.5 mL MNPs carrying 0.4 mg NIPA-M was injected into the ARGP via a 25-gauge needle attached to a polyethylene tube as previously described.[9] The maximal sinus rate slowing response induced by ARGP stimulation without causing AF was measured in the baseline state and 30 minutes, 60 minutes, 2 hours, and 3 hours after MNP injection into the ARGP. In 4 other animals, a cylindrical permanent magnet (2600 G; surface area, 2 cm^2) was sutured to the epicardial surface of the fat pad containing the IRGP but not the ARGP to capture the MNPs. The circumflex coronary artery was cannulated, and 1 mL MNPs that contained ≈0.8 mg NIPA-M was infused into the circumflex coronary artery over 3 to 4 minutes. Both the ARGP function and IRGP function as described above were assessed at the time intervals of 30, 60, 90, and 120 minutes.

Two sets of control experiments were conducted in 7 additional animals: set 1, MNPs containing the magnetic core and hydrogel shell but without the NIPA-M payload (n=4) were targeted to determine whether suppression of the IRGP function occurred in the absence of NIPA-M with microembolization alone; set 2, nanoparticles made of the hydrogel shell and NIPA-M payload but without the magnetic core (n=3) were infused to assess whether magnetic targeting was essential for effecting AF inducibility. All control animals received transcoronary delivery of the nanoparticles, and electrophysiological studies were performed before and after the interventions.

In 6 other animals, 1.6 mg NIPA-M (twice the amount of NIPA-M incorporated into 1 transcoronary delivery) was directly injected into the left ventricle. NIPA-M used in these experiments was not

incorporated into the hydrogel to simulate the greatest possible toxic challenge should the total NIPA-M dose be released instantly into the circulation from transcoronary infusion. Serum samples before and 9.7±0.3 hours after NIPA-M injection were collected for paired analysis to assess renal and hepatic toxicity.

Histological Studies

In the experimental group, in 3 of 4 dogs receiving MNP infusion into the circumflex artery, both the ARGP and IRGP and adjacent atrial tissue were excised for histological confirmation of targeted drug delivery to the IRGP. In the control group (MNP without NIPA-M payload), IRGP and adjacent atrial tissue were excised for histological iron stain confirmation of targeted delivery to the IRGP. GP and atrial tissue were fixed in formalin and embedded in paraffin. Serial sections of the entire tissue block were performed. Prussian Blue stain was used to detect both ferric and ferrous salts that form the core of the MNP.

Statistical Analysis

All data are presented as mean±SE. The changes in GP function and AF threshold induced by GP stimulation at different time courses were evaluated by repeated-measures ANOVA followed by the Tukey test for comparing different time points after the application of MNP versus baseline. All data were evaluated by the GraphPad Prism version 5.0 software (GraphPad Software, Inc, San Diego, CA). All analyses were 2 tailed. Statistical significance was defined as $P<0.05$.

Results

Physical Properties of the Core-Shell Magnetic Nanoparticles

The average size of the functionalized MNPs was determined by transmission and scanning electron micrograph. The average MNP coated with pNIPA-AAm was ≈100 nm in diameter. Figure 2A shows that each magnetic core (dark center) was surrounded by a polymeric shell layer (white layer surrounding the dark core). For drug-loading studies, NIPA-M was added at a concentration of 2.5 mg/mL to the nanoparticle suspension as described in the Methods section. The loading efficiency of NIPA-M was found to be 38%, consistent with the previously described efficiency.[25,26]

The release kinetics at both 25°C and 37°C followed a parallel curvilinear course. Cumulative release of NIPA-M at 37°C was approximately twice as much as that at 25°C. Importantly, nearly 30% of the NIPA-M was released within the first 2 hours at 37°C (inset in Figure 2B).

Microinjection of MNPs Into the ARGP

To examine the in vivo neurotoxic effect of the MNPs, 0.5 mL MNPs containing 0.4 mg NIPA-M was injected into the ARGP as described above. Figure 3 (left) shows the percent of maximal sinus rate slowing caused by ARGP stimulation without inducing AF. Before MNP injection, ARGP stimulation reduced the sinus rate by 40±8%, whereas 2 hours after MNP injection, ARGP stimulation only exerted a maximal effect of 21±9% ($P=0.006$). The lowest voltage (threshold) of ARGP stimulation that induced AF was increased from 5.9±0.8 V (baseline) to 10.2±0.9 V (2 hours; $P=0.009$). The effects of ARGP suppression did not differ between 2 and 3 hours after MNP injection (data not shown). Therefore, subsequent experiments were conducted up to 2 hours after intracoronary infusion of the MNPs.

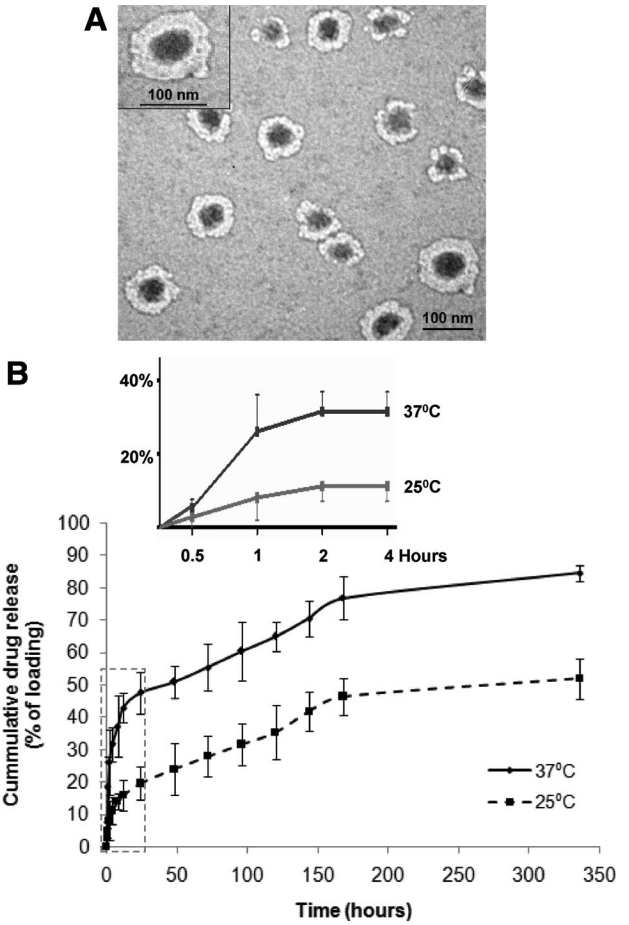

Figure 2. Physical properties of the MNP. A, Transmission electron micrograph of pNIPA-AAm–coated MNPs. Each magnetic core (dark center) was surrounded by a polymeric shell layer (white layer surrounding the dark core). B, In vitro release profiles of NIPA-M from pNIPA-AAm–coated MNPs at 25°C and 37°C. Curves represent the cumulative percent releases of NIPA-M over 336 hours at 25°C and 37°C. Inset, Release kinetics in the first 4 hours indicated by the dotted box in B.

Intracoronary Arterial Delivery of MNPs

In the 4 animals receiving infusion of the MNPs into the circumflex coronary artery, the ARGP and IRGP functions were measured before and after MNP infusion. Before the administration of the MNP, IRGP stimulation during AF slowed the ventricular rate by 57±8%, but this effect was diminished to 33±3% ($P=0.034$) and 20±8% ($P=0.002$) 1.5 and 2 hours after infusion of the MNPs, respectively (Figure 4A). In contrast, the sinus rate slowing response induced by stimulation of the ARGP, where no magnet was placed, was not altered over a period of 2 hours (31±7% at baseline, 33±8% at 2 hours; $P=0.604$).

In the 4 animals receiving MNPs without NIPA-M payload and the 3 animals receiving nanoparticles without the magnetic core, the IRGP function was not altered over 3 hours (Figure 4C and 4D). In the 6 animals the receiving NIPA-M direct ventricular injection, the serum creatine, blood urea nitrogen (BUN), ratio of BUN to creatine, and alanine aminotransferase did not change (before NIPA-M: creatinine=0.8±0.1 mmol/L, BUN=14.8±3.4 mmol/L, ratio of BUN to creatine=19.1±4.7, alanine aminotransfer-

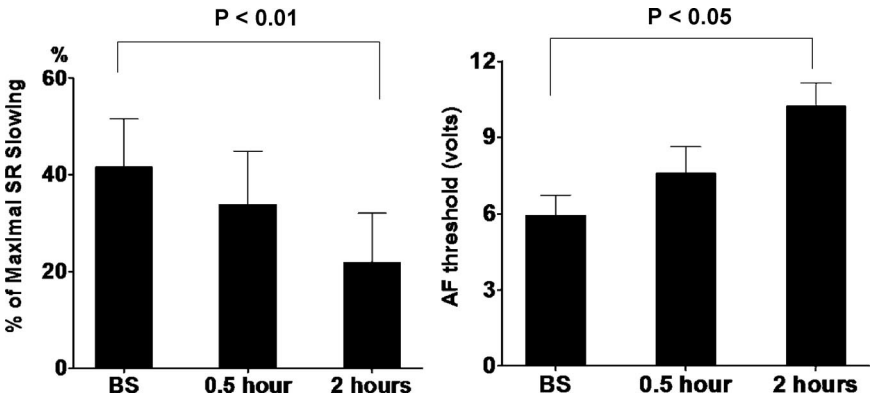

Figure 3. Microinjection of MNPs carrying 0.4 mg NIPA-M into the ARGP (N=6). Left, Two hours after the injection, the maximal decrease in sinus rate by ARGP stimulation was reduced from 40±8% to 21±9%. Right, AF threshold also significantly increased 2 hours after injection. BS indicates baseline.

ase=33.3±5.6 U/L; at 9.7±0.3 hours after NIPA-M: creatine=0.9±0.1 mmol/L, BUN=16.2±2.9 mmol/L, ratio of BUN to creatine=17.6±1.7, alanine aminotransferase =41.3±8.7 U/L; $P>0.05$ for all by paired t test).

Histological studies demonstrated small Prussian Blue–positive aggregates in the epicardial fat pad containing the IRGP but not the ARGP (Figure 5A and 5B). In addition, large Prussian Blue–positive aggregates were found only in the microcirculation of the IRGP and not in the ARGP, implying embolization of the microcirculation of the IRGP by these large MNP aggregates (Figure 5C and 5D).Figure 5E and 5F shows small Prussian Blue–positive aggregates in the epicardial fat pad containing the IRGP in the control group (MNPs without NIPA-M payload) as well. In contrast, only rare and faint Prussian Blue–positive reactions were found after serial histological sections of the ARGP were carefully examined (data not shown).

Discussion

Main Findings

In this study, we demonstrated that GP function can be suppressed by a novel targeted drug delivery system composed of magnetite (core), thermoresponsive pNIPA-AAm hydrogel matrix (shell), and NIPA-M (neurotoxin) payload. Electrophysiological and histological studies verified that the external magnetic force was capable of pulling these MNPs out of the microcirculation and inhibiting the function of the targeted neural tissue. To the best of our knowledge, this is the first report in which targeted MNPs were used in an attempt to treat cardiac arrhythmia.

Nanoparticles with superparamagnetic behavior have attracted clinical attention for drug delivery for their unique property that they magnetize strongly in the presence of an external magnetic field but retain no permanent magnetism after the magnetic field is removed.[18,33] Such nanoparticles carrying therapeutic agents can potentially be encompassed and concentrated into the targeted tissue for a controlled period of time to allow targeted therapy with minimal systemic side effects. Thermoresponsive hydrogel based on pNIPA-AAm had been synthesized and functionalized for >2 decades.[34] At temperatures above the lower critical solution temperature, pNIPA-AAm hydrogel shrinks by expelling water molecules and releasing the payload molecules incorporated into the hydrogel. In the present study, we success-

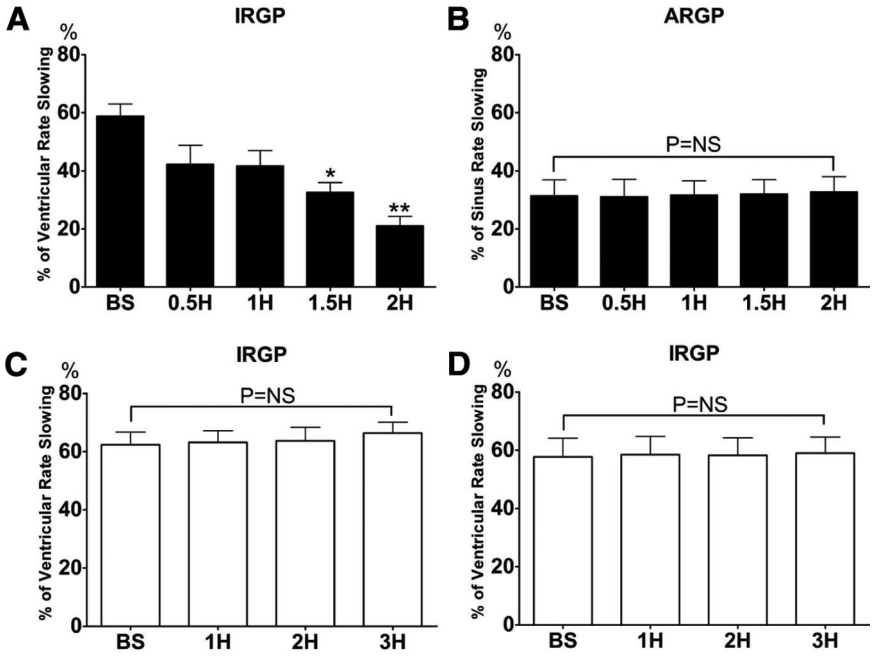

Figure 4. Changes in the GP function after infusion of MNPs into the circumflex coronary artery. A and B, MNPs carrying 0.8 mg NIPA-M (magnet was attached to the IRGP but not ARGP; n=4). The maximal ventricular rate slowing response induced by IRGP stimulation during AF was reduced from 57±8% (baseline [BS]) to 33±3% (1.5 hours; $P<0.05$) and 20±8% (2 hours; $P<0.01$). In contrast, the ARGP function, assessed by the maximal sinus rate slowing response induced by ARGP stimulation, was not altered. C and D, Control experiments. After the magnet was attached to the IRGP, the animals received transcoronary infusion of MNPs without NIPA-M (C; n=4) or nanoparticles without the magnetic core (D; n=3). *$P<0.05$, **$P<0.01$ vs baseline in A.

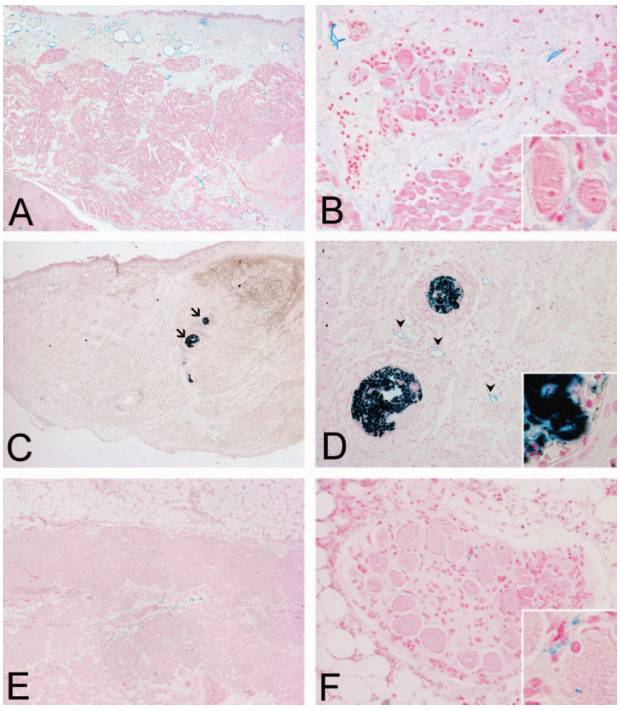

Figure 5. Representative examples of the IRGP histology after intracoronary arterial infusion of MNP. A, On low magnification, a small amount of iron (blue staining) is present, most notably in subepicardial adipose tissue. B, Blue MNP aggregations are also present in ganglia. Most of the iron depositions are present in the periganglionic tissue (inset). C, Intravascular emboli (arrows) containing iron are present in some of the sections. D, On high magnification, iron depositions are also present in the adipose tissue (arrowheads) around the blood vessels. High magnification of the iron-containing thrombus is shown in the inset. E, Similar iron depositions are noted in the adipose tissue of the control heart. High magnification of the deposits is shown in the inset. F, Iron depositions are also present in the ganglions of control heart. Original magnification for A, C, and E, ×4; for B, D, and F, ×20; for the insets, ×60.

fully synthesized MNPs that had a lower critical solution temperature at 37°C. The release kinetic study showed that ≈30% of the NIPA-M was released from the pNIPA-AAm hydrogel in the first 2 hours (Figure 2B). Significant suppression of the targeted IRGP function was achieved 2 hours after intracoronary infusion of the MNP. Although we were not capable of tracking the movement of individual MNP and the in vivo release kinetics of the NIPA-M was not investigated, the sharp contrast of the effects on the ARGP and IRGP function indicated that the MNPs were successfully targeted to the IRGP and that sufficient NIPA-M was released within the IRGP to cause neurotoxicity and suppression of the IRGP function. It is possible that microvascular embolization by MNP aggregates also may contribute to the effect.

Multiple basic studies have demonstrated the significant impact on AF after the major left atrial GP were ablated. Using a rapid atrial pacing model, Lu et al[10] showed that shortening of the effective refractory period, increase of effective refactory period dispersion, and increased AF inducibility caused by rapid atrial pacing for 3 hours were all reversed by ablation of the 4 major atrial GP and ligament of Marshall. In animals receiving GP ablation first, rapid atrial pacing for 6 hours failed to change the effective refractory period, effective refactory period dispersion, and AF inducibility. The authors proposed that autonomic denervation may serve as a therapeutic modality to prevent paroxysmal AF from progressing to more persistent forms of AF. Other studies also demonstrated that after ablation of the GP and ligament of Marshall, AF became more difficult to initiate and sustain; regularization of the fractionated potentials often led to the termination of AF after GP ablation.[11,35] Moreover, GP ablation may also convert AF from the focal form of AF to the macroreentrant form of AF, which was more responsive to antiarrhythmic drugs.[35]

Several clinical studies also indicated the benefits of autonomic denervation by targeting the major atrial GP identified by high-frequency stimulation similar to what was described in the present study. When GP ablation was combined with PV isolation, the success rate improved.[12–14] Despite the observations that AF remained inducible after GP ablation, addition of PV isolation produced a long-term success rate of >90% in patients with paroxysmal AF.[12,14] A series of recent articles by Pokushalov and colleagues[15–17] also reported similar success rates in AF ablation targeting only the major atrial GP compared with the standard PV isolation approach. Because GP ablation alone does not require PV isolation, these results not only challenge the conventional wisdom that PV isolation is a necessity for the success of AF ablation but also underscore the important contribution of the intrinsic cardiac autonomic nervous system, particularly the GP, to the dynamics of AF initiation and maintenance. In the present study, the idea of using targeted drug delivery to treat AF was also built on this concept.

Neurotoxins such as botulinum toxin (ie, BOTOX) have been used to treat various local diseases with minimal systemic side effects.[36,37] Monomers of acrylamide and its analogs, including NIPA-M, have a long history of producing systemic neurotoxicity in humans and experimental animals. Neuropathological studies suggested that acrylamide neurotoxicity was related to inhibition of glycolytic enzymes such as enolase, leading to toxic effects on both neurons and axons.[38–40] In the present study, the IRGP function was significantly suppressed by a single intracoronary infusion that contained 0.8 mg NIPA-M that was ≈7 mmol/L (0.8 mg in 1 mL; molecular weight=113). The LD_{50} of NIPA-M to kill 50% neurons was 5 to 8 mmol/L.[41] Our histological evidence showed that epicardial fat and GP contained the greatest concentration of MNP, suggesting that the concentration of NIPA-M in the GP would be much higher than the LD_{50}. This may explain the finding that significant suppression of the GP function was observed 2 hours after intracoronary infusion of the MNP. NIPA-M has also been reported to induce clinical (ataxia, rotorod performance deficits) and morphological (tibial nerve degeneration) signs of neuropathy after prolonged oral exposure (ie, 2.65 mmol/L in drinking water for 90 days or ≈20 $mg \cdot kg^{-1} \cdot d^{-1}$).[40–42] Lower dosing rates (1 to 20 $mg \cdot kg^{-1} \cdot d^{-1}$) typically require 60 days to 2 years to elicit overt and morphological signs of neuropathy.[40–42] In the present study, with an average body weight of dogs of 20 to 25 kg, this would result in a single exposure to NIPA-M of ≈0.04 mg/kg. If NIPA-M were

slowly released back into the circulation from the targeted GP, the concentration of the NIPA-M would be far below the threshold for inducing any systemic neurotoxicity. Moreover, the present study was designed using a single application of the MNP to destroy the autonomic neurons concentrated in the GP, which do not regenerate, further lowering the risks associated with prolonged exposure to NIPA-M. Importantly, our proof-of-concept study provides experimental evidence supporting the idea of magnetic targeted drug delivery to ablate the GP. It is foreseeable that other agents such as pharmaceuticals or toxins with even less potential side effects may be incorporated into the hydrogel matrix as the payload.

Clinical Implications

AF is the most commonly encountered cardiac arrhythmia, affecting 2.5 million people in the United States. As the population ages, the incidence is projected to increase to 6 million in the year 2029, a significant portion of whom will have drug-refractory AF and require ablation.[43] Catheter or surgical ablation carries significant risks of serious complications and is very costly. Targeted drug delivery as described in the present study provides a less invasive and less expensive therapeutic modality. With the advances in stereotactic localization by an externally applied magnetic field, it is possible to selectively deliver the MNPs to multiple GP to achieve autonomic denervation and to treat AF without the risks of serious complications associated with catheter or surgical ablation or the side effects from long-term antiarrhythmic therapy.

Study Limitations

Although we have provided both electrophysiological and histological evidence supporting the conclusion that suppression of the targeted GP function was caused by release of the payload neurotoxin, the kinetics of the mobilization of the MNP from the intravascular space to the epicardium remains unquantified because doing so would require the excision of the targeted GP at different time intervals. In addition, the kinetics of payload release in vivo was not studied. Taken together, the minimal duration for the external magnetic force that needs to be applied to capture the MNP within the target tissue and to release the payload remains unclear.

Prior studies have demonstrated that AF inducibility was not reduced or was even increased if ablation was limited to only 1 or 2 GP.[44,45] This paradoxical effect may result from increased dispersion of refractoriness caused by ablating only 1 or 2 GP. Therefore, AF inducibility before and after targeted MNP delivery was not evaluated in this study. Changes in global AF inducibility will need to be tested in the future with the external magnetic force applied to all the major atrial GP.

Conclusions

Intravascularly administered MNPs carrying NIPA-M can be magnetically targeted to the IRGP and reduce GP activity presumably by the subsequent release of NIPA-M. This novel targeted drug delivery system can be used intravascularly for targeted autonomic denervation. With the advances in stereotactic localization of externally applied magnetic field, this novel approach may serve as a less invasive and less expensive therapeutic modality to treat drug-refractory AF.

Acknowledgments

We thank Andrea Moseley and Dr Tushar Sharma for their technical assistance in the experimental studies. We also thank H. Greg Matlock and Howard Doughty for their careful preparation of the histological slides.

Sources of Funding

This work was supported in part by a grant from the College of Medicine Alumni Association of the University of Oklahoma (Dr Po) and by the Helen and Will Webster Arrhythmia Research Fund.

Disclosures

Dr Scherlag has received a research grant from St Jude Medical and has served as a consultant to Atricure, Inc and Symphony Medical. Dr Pope has received research grants and served as a grant reviewer for the National Institutes of Health, has been an expert witness for Farnam versus Farnam and Wrather versus Farnam, and is a consultant to the US Environmental Protection Agency. Dr Po has received a research grant from the College of Medicine Alumni Association of the University of Oklahoma and honoraria from St Jude Medical and Johnson & Johnson, in addition to being a consultant for Atricure, Inc. The other authors report no conflicts.

References

1. Bettoni M, Zimmermann M. Autonomic tone variations before the onset of paroxysmal atrial fibrillation. *Circulation*. 2002;105:2753–2759.
2. Amar D, Zhang H, Miodownik S, Kadish A. Competing autonomic mechanisms precedes the onset of postoperative atrial fibrillation. *J Am Coll Cardiol*. 2003;42:1262–1268.
3. Ogawa M, Zhou S, Tan AY, Song J, Gholmieh G, Fishbein MC, Lou H, Siegel RJ, Karagueuzian HS, Chen LS, Lin SF, Chen PS. Left stellate ganglion and vagal nerve activity and cardiac arrhythmias in ambulatory dogs with pacing-induced congestive heart failure. *J Am Coll Cardiol*. 2007;50:335–343.
4. Patterson E, Po SS, Scherlag B, Lazzara R. Triggered firing in pulmonary veins initiated by in vitro autonomic nerve stimulation. *Heart Rhythm*. 2005;2:624–631.
5. Randall WC, Armour JA, Geis WP, Lippincott DB. Regional cardiac distribution of the sympathetic nerves. *Fed Proc*. 1972;31:1199–1208.
6. Ardell JL. Structure and function of the mammalian intrinsic cardiac neurons. In: Armour JA, Ardell JL, eds. *Neurocardiology*. New York, NY: Oxford University Press; 1994; chap. 5.
7. Pauza DH, Skripka V, Pauziene N. Morphology of the intrinsic cardiac nervous system in the dog: a whole-mount study employing histochemical staining with acetylcholinesterase. *Cells Tissues Organs*. 2002; 172:297–320.
8. Scherlag BJ, Yamanashi WS, Patel U, Lazzara R, Jackman WM. Autonomically induced conversion of pulmonary vein focal firing into atrial fibrillation. *J Am Coll Cardiol*. 2005;45:1878–1886.
9. Po SS, Scherlag BJ, Yamanashi WS, Edwards J, Zhou J, Wu R, Geng N, Lazzara R, Jackman WM. Experimental model for paroxysmal atrial fibrillation arising at the pulmonary vein-atrial junctions. *Heart Rhythm*. 2006;3:201–208.
10. Lu Z, Scherlag BJ, Lin J, Niu G, Fung KM, Zhao L, Ghias M, Jackman WM, Lazzara R, Jiang H, Po SS. Atrial fibrillation begets atrial fibrillation: autonomic mechanism for atrial electrical remodeling induced by short-term rapid atrial pacing. *Circ Arrhythm Electrophysiol*. 2008;1: 184–192.
11. Lin J, Scherlag BJ, Zhou J, Lu Z, Patterson E, Jackman WM, Lazzara R, Po SS. Autonomic mechanism to explain complex fractionated atrial electrograms (CFAE). *J Cardiovasc Electrophysiol*. 2007;18:1197–1205.
12. Po SS, Nakagawa H, Jackman WM. Localization of left atrial ganglionated plexi in patients with atrial fibrillation. *J Cardiovasc Electrophysiol*. 2009;20:1186–1189.
13. Scherlag BJ, Nakagawa H, Jackman WM, Yamanashi SW, Patterson E, Po S, Lazzara R. Electrical stimulation to identify neural elements on the heart: their role in atrial fibrillation. *J Interv Card Electrophysiol*. 2005; 13:37–42.

14. Danik S, Neuzil P, Avila A, Malchano ZJ, Kralovec S, Ruskin JN, Reddy VY. Evaluation of catheter ablation of periatrial ganglionic plexi in patients with atrial fibrillation. *Am J Cardiol*. 2008;102:578–583.
15. Pokushalov E, Romanov A, Shugayev P, Artyomenko S, Shirokova N, Turov A, Katritsis DG. Selective ganglionated plexi ablation for paroxysmal atrial fibrillation. *Heart Rhythm*. 2009;6:1257–1264.
16. Pokushalov E, Turov A, Shugayev P, Artyomenko S, Romanov A, Shirokova N. Catheter ablation of left atrial ganglionated plexi for atrial fibrillation. *Asian Cardiovasc Thorac Ann*. 2008;16:194–201.
17. Pokushalov E. The role of autonomic denervation during catheter ablation of atrial fibrillation. *Curr Opin Cardiol*. 2008;23:55–59.
18. Neuberger T, Schöpf B, Hofmann H, Hofmann M, Rechenberg BV. Superparamagnetic nanoparticles for biomedical applications: possibilities and limitations of a new drug delivery system. *J Magn Magn Mater*. 2005;293:483–496.
19. Corot C, Robert P, Idee JM, Port M. Recent advances in iron oxide nanocrystal technology for medical imaging. *Adv Drug Deliv Rev*. 2006; 58:1471–1504.
20. Ito A, Shinkai M, Honda H, Kobayshi T. Medical application of functionalized magnetic nanoparticles. *J Biosci Bioeng*. 2005;100:1–11.
21. Kim J, Lee JE, Lee SH, Yu JH, Lee JH, Park TG, Hyeon T. Designed fabrication of a multifunctional polymer nanomedical platform from simultaneous cancer-targeted imaging and magnetically guided drug delivery. *Adv Mater*. 2008;20:478–483.
22. Dormer K, Seeney C, Lewelling K, Lian G, Gibson D, Johnson M. Epithelial internalization of superparamagnetic nanoparticles and response to external magnetic field. *Biomaterials*. 2005;26:2061–2072.
23. Gupta AK, Gupta M. Synthesis and surface engineering of iron oxide nanoparticles for biomedical applications. *Biomaterials*. 2005;26:3995–4021.
24. Rahimi M, Youself M, Cheng Y, Meletis EI, Eberhart RC, Nguyen KT. Formulation and characterization of covalently coated magnetic nanogel. *J Nanosci Nanotechnol*. 2009;9:4128–4134.
25. Rahimi M, Kilaru S, El Hajj Sleiman G, Saleh A, Rudkevich D, Nguyen KT. Synthesis and characterization of thermo-sensitive nanoparticles for drug delivery applications. *J Biomed Nanotechnol*. 2008;4:482–490.
26. Salehi R, Arsalani N, Davaran S, Entezami AA. Synthesis and characterization of thermosensitive and pH-sensitive pol (N-isopropylacrylamide-acrylamide-vinylpyrrolidone) for use in controlled release of naltrexone. *J Biomed Mater Res A*. 2009;89:919–928.
27. Wakamatsu H, Yamamoto K, Nakao A, Aoyagi T. Preparation and characterization of temperature-responsive nanoparticles conjugated with N-isopropylacrilamide-based functional copolymer. *J Magn Magn Mater*. 2006;302:327–333.
28. Wadajkar A, Koppolu B, Rahimi M, Nguyen KT. Cytotoxic evaluation of N-isopropylacrylamide monomers and temperature-sensitive poly(N-isopropylacrylamide) nanoparticles. *J Nanopart Res*. 2009;11: 1375–1382.
29. Chastek T, Wadajkar A, Nguyen KT, Hudson SD, Chastek T. Polyglycol-templated synthesis of poly(N-isopropyl acrylamide) microgels with improved biocompatibility. *Colloid Polym Sci*. 2010;288:105–114.
30. Zhou J, Scherlag BJ, Edwards J, Jackman WM, Lazzara R, Po SS. Gradients of atrial refractoriness and inducibility of atrial fibrillation due to stimulation of ganglionated plexi. *J Cardiovasc Electrophysiol*. 2007; 18:83–90.
31. Hou Y, Scherlag BJ, Lin J, Lu Z, Truong K, Patterson E, Lazzara R, Jackman W, Po SS. Ganglionated plexi modulating extrinsic cardiac autonomic nervous inputs: effects on sinus rate, AV conduction, refractoriness and AF inducibility. *J Am Coll Cardiol*. 2007;50:61–68.
32. Hou Y, Scherlag BJ, Zhou J, Song J, Patterson E, Lazzara R, Jackman WM, Po SS. Interactive atrial neural network: determining the connections between ganglionated plexi. *Heart Rhythm*. 2007;4:56–63.
33. Asmatulu R, Zalich MA, Claus RO, Riffle JS. Synthesis, characterization and targeting of biodegradable magnetic nanocomposite particles by external magnetic fields. *J Magn Magn Mater*. 2005;292:108–109.
34. Pelton R. Temperature-sensitive aqueous microgels. *Adv Colloid Interface Sci*. 2000;85:1–33.
35. Niu G, Scherlag BJ, Lu Z, Ghias M, Zhang Y, Patterson E, Dasari TW, Zacharias S, Lazzara R, Jackman WM, Po SS. An acute experimental model demonstrating 2 different forms of sustained atrial tachyarrhythmias. *Circ Arrhythm Electrophysiol*. 2009;2:384–392.
36. Brashear A. The safety and tolerability of botulinum toxin for the treatment of cervical dystonia. *Expert Opin Drug Saf*. 2005;4:241–249.
37. Brin MF. Development of future indications for BOTOX. *Toxicon*. 2009; 54:668–674.
38. Tanil H, Hashimoto K. Effect of acrylamide and related compounds on glycolytic enzymes of rat brain. *Toxicol Lett*. 1985;26:79–84.
39. Howland RD. The etiology of acrylamide neuropathy: enolase, phosphofructokinase and glyceraldehyde-3-phosphotase dehydrogenase activities in peripheral nerve, spinal cord, brain and skeletal muscle of acrylamide-intoxicated cats. *Toxicol Appl Pharmacol*. 1981;60:324–333.
40. LoPachin RM. Acrylamide neurotoxicity: neurological, morphological and molecular endpoints in animal models. *Adv Exp Med Biol*. 2005;561: 21–37.
41. LoPachin RM, Ross JF, Reid ML, Das S, Mansukhani S, Lehning EJ. Neurological evaluation of toxic axonopathies in rats: acrylamide and 2,5-hexanedione. *Neurotoxicology*. 2002;23:95–110.
42. Lopachin RM, Gavin T. Acrylamide-induced nerve terminal damage: relevance to neurotoxic and neurodegenerative mechanisms. *J Agric Food Chem*. 2008;56:5994–6003.
43. Benjamin EJ, Wolf PA, D'Agostino RB, Silbershatz H, Kannel WB, Levy D. Impact of atrial fibrillation on the risk of death: the Framingham Heart Study. *Circulation*. 1998;98:946–952.
44. Hirose M, Leatmanoratn Z, Laurita KR, Carlson MD. Partial vagal denervation increases vulnerability to vagally induced atrial fibrillation. *J Cardiovasc Electrophysiol*. 2002;13:1272–1279.
45. Oh S, Zhang Y, Bibevski S, Marrouche NF, Natale A, Mazgalev TN. Vagal denervation and atrial fibrillation inducibility: epicardial fat pad ablation does not have long-term effects. *Heart Rhythm*. 2006;3:701–708.

CLINICAL PERSPECTIVE

The intrinsic cardiac autonomic nervous system, composed of ganglionated plexi and interconnecting nerves, is involved in the initiation of atrial fibrillation. Injury of ganglionated plexi (GP) may be important for the success of atrial fibrillation ablation in some patients but with present catheter methods, success is achieved with substantial ablation to atrial myocardium. In this animal investigation, we show the feasibility of a targeted drug delivery system for GP ablation. Superparamagnetic nanoparticles containing magnetite, a hydrogel matrix, and a neurotoxin were synthesized. When injected into a ganglia, the neurotoxin is released and suppresses GP function. When a magnet is placed over a GP, superparamagnetic nanoparticles injected into a coronary artery concentrate in the GP beneath the magnet and suppress GP function. With the advances in stereotactic localization, it may be possible to use externally applied magnetic fields to target GP for ablation with superparamagnetic nanoparticles.